General description of cold sprayed coatings formation and of their properties

M. WINNICKI*, T. PIWOWARCZYK, and A. MAŁACHOWSKA

Wrocław University of Science and Technology, Faculty of Mechanical Engineering, 5/7 Łukasiewicza St., 50-370 Wrocław, Poland

Abstract. This paper intends to describe the formation of cold sprayed coatings and their properties based on latest works. Thermodynamic aspects of the cold spray process are discussed, including the main factors influencing powder particles velocity, e.g. nozzle construction, gas type, powder morphology as well as its significance for coating quality. The phenomenon of coating building is illustrated using both numerical simulation and microstructure analysis. Particular emphasis is placed on the description of critical and erosion velocities. Microstructure and coating properties have also been discussed, i.e. porosity, electrical conductivity and residual stresses based on own research. These are further supplemented by a literature review. Finally, clear division between the low and high pressure cold spray method is made.

Key words: bonding mechanism, microstructure, FEM, high pressure cold spray, low pressure cold spray.

1. Introduction

In the last four decades there has been a change in the thermal-spraying trend, which focused on higher kinetic energies of particles. This facilitates particles deformation without high temperature, allowing to achieve significant benefits, such as forming clean and dense coatings with little oxidation. The cold gas spraying (CGS) method is the latest among the thermal-spraying ones. Its main advantages include high efficiency of the spraying process, small residual stresses in the coating, small amount of heat introduced into the substrate, phase stability (no transformations), reduction of porosity (greater deformation of particles), significant reduction in coating oxidation and also in most cases a lack of need for masking the substrate. In addition, the temperature of the process is much lower than the melting point of the material used, which eliminates the phenomenon of powder particles melting in the stream. Residual stresses occurring in the coating are of a compressive nature, which is due to the compaction of the particles impacting the solid state. The deposition process in the cold spray requires certain ductility of materials, therefore mostly metals and mixtures of metals and ceramics are applied as feedstock materials [1, 2].

2. Velocity of particles during spraying

In the cold spray method, the powder particles obtain very high velocities, impact the substrate with a high kinetic energy and, as a result, deform and adhere to the substrate or previously deposited particles. Building a coating is possible thanks to a nozzle with a special converging-diverging shape, which is known as de Laval nozzle. In it, working gas (air, nitrogen, helium or their mixtures) achieves supersonic velocity and then transfers it to the powder particles by means of the drag force [1, 3–7]. Hence, powder deposition is dependent on particle velocity. The dynamics of the gas affects both the velocity of the particles and their temperature. Meanwhile, gas velocity depends both on its pressure and temperature at the entrance to the nozzle. However, it is more significantly influenced by the gas temperature than by its pressure [8]. An increase in the temperature of the gas simultaneously increases the velocity and temperature of the powder [9, 10]. In the converging part of the nozzle, just before the throat, temperature and pressure decrease while velocity slightly increases. In the throat of the nozzle velocity of the gas increases and reaches the maximum value in the diverging part during expansion of the gas, with a simultaneous sharp decline in the values of temperature and pressure (Fig. 1).

Depending on the system, the powder is introduced into the converging part or directly after the throat of the nozzle, which enables it to acquire velocity and temperature from the gas
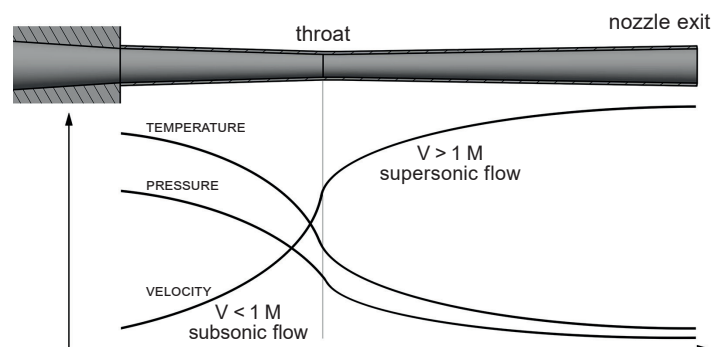

Fig 1. Diagram of de Laval nozzle together with flow characteristics: velocity, temperature and pressure (inspired by [14])

*e-mail: marcin.winnicki@pwr.edu.pl

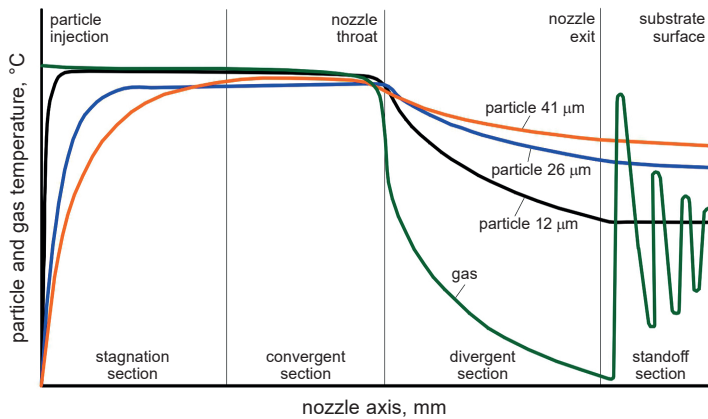M. Winnicki, T. Piwowarczyk, and A. Małachowska

Fig 2. Gas and powder temperature inside and outside the de Laval nozzle (inspired by [15])

(Fig. 3, 4, respectively) [4, 11, 12]. Additionally, it is also possible to heat the powder before spraying, which increases its plasticity [13]. At the nozzle exit the gas has a higher velocity than the particles but its temperature is also lower [5, 11, 14].

Outside the de Laval nozzle, two areas with a shockwave are formed in the gas stream. One occurs immediately after
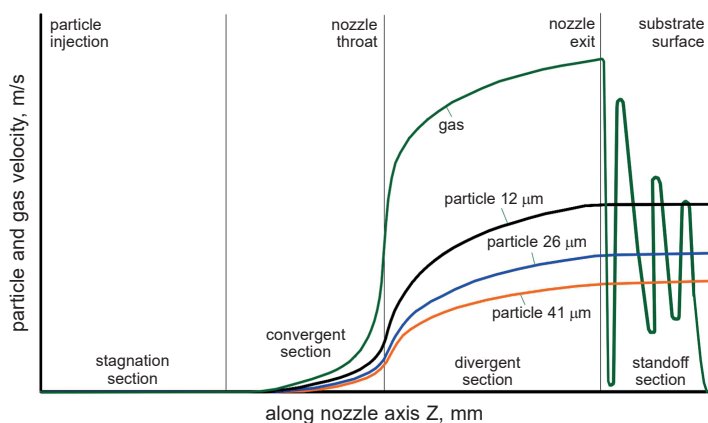

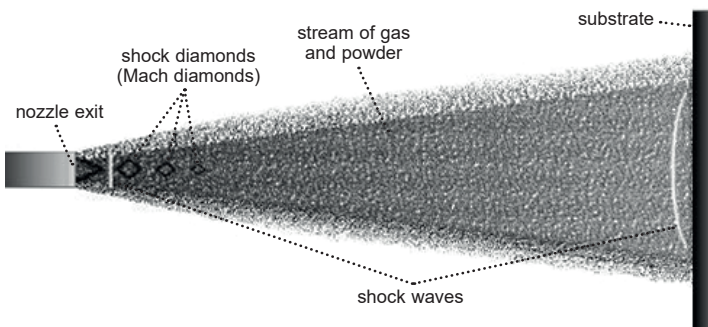Fig 3. Gas and powder velocity inside and outside the de Laval nozzle (inspired by [15])

Fig. 4. Supersonic stream diagram (own materials)

the exit from the nozzle, where the pressure and temperature of the gas adjust themselves to the ambient parameters. The second one (bow shock), which has a much greater impact on the process of spraying, occurs at the surface in the form of an arc (Fig. 4). It results from deceleration and deflection of the flow in front of the substrate and creates the high pressure and density gas layer. This is accompanied by an increase in gas temperature.

Particle velocity decreases in the second shock wave because of increased gas density and increased drag force [12, 16, 17]. Therefore, the powder particles should have enough velocity to break through the bow shock. On the other hand, the drag coefficient is lower for spherical particles as compared to irregular particles. As a result, in the gas stream irregular particles with a large drag force demonstrate higher velocities [18, 19].

2.1. Critical velocity. A parameter known as critical velocity v_{cr} has been defined for sprayable materials. It stands for the velocity above which the particles adhere to the substrate as a result of plastic deformation (Fig. 5). For velocities lower than critical velocity, the particles bounce off the substrate, constituting a loss of material and activating the substrate by cleaning it from oxides at the same time [5–7, 11, 20, 21]. In the case of very high velocities, the particles dig into the substrate, leading to its erosion. Therefore a definition of a second critical velocity was introduced, known as erosion velocity v_{er}. Critical velocity is dependent on several parameters, i.e. the material and temperature of the powder and the substrate, granulation, shape and oxidation of the powder, as well as the preparation
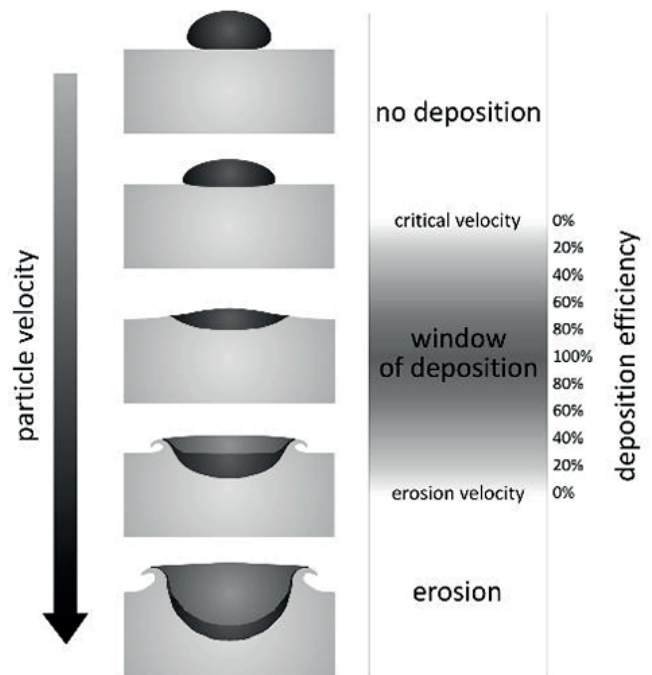

Fig. 5. Influence of particle velocity on deposition efficiency (inspired by [13])

of the substrate [7, 22]. In addition, critical velocity v_{cr} and erosion velocity v_{er} decrease along with an increase in the temperature of the particles, deoxidation of the particles and activation of the substrate [7, 11]. In contrast, velocity of a single powder particle will be determined by the size and density of the particle, the temperature and pressure of the gas, the type of working gas (molecular weight and adiabatic exponent) and the geometry of the nozzle. Higher gas temperature causes an increase in viscosity, increasing gas velocity and thereby also powder particles velocity [23]. Moreover, all of these parameters have a crucial impact on the formation of coatings and the efficiency of spraying [3, 5, 24]. However, both the parameters and properties of the gas turn out to be crucial. It turns out that a lower molar mass of the gas allows for obtaining greater velocities [6, 11]. Gases typically used in the cold spray process include air, nitrogen and helium. The molar mass of air and N_2 is, respectively, 29 g/mol and 28 g/mol, and for He it is 4 g/mol [25]. In contrast, the adiabatic exponent for monoatomic gases (He) is 1.66 and for diatomic gases (N_2 or air) it is 1.4. A higher adiabatic exponent allows for achieving higher velocities [3]. In addition, the speed of sound is 343 m/s for air, 349 m/s for nitrogen, and 989 m/s for helium. These properties indicate that using helium as a working gas in the process of cold spraying allows for obtaining the highest velocities, twice exceeding the speed of nitrogen [11, 26]. However, the use of helium for industrial purposes is limited, due to the enormous costs of its exploration. It is possible to use a system of recovery but this involves higher investment outlays.

If the powder used in the process has a wide range of particle size distribution, critical velocity is determined for the largest particles, because the fine particles have a higher velocity [7, 27]. Particle velocity decreases along with the increase of their size, which results in smaller deformation upon impact onto the substrate [28]. On the other hand, small particles are more oxidized in relation to their volume and a thicker layer of oxide on the powder particles requires higher critical velocity for the particles to be deposited in the coating [29]. In the development of the issue of critical velocity, various equations for calculation of this parameter were determined. The results of calculations of both critical velocity and erosion velocity for individual material are described in [13].

3. Mechanism of coating formation

In the cold spray method, the first powder particles in the stream hit the oxide layer, covering the substrate, as a result of which they do not reach critical velocity [6, 30]. Upon hitting the substrate, the particles bounce off it, causing the formation of craters and breakdown of the oxide layer. Subsequent particles begin to form the proper coating as a result of contact with a clean substrate (Fig. 6). In the cold spraying process, the formation of the coating takes place in two stages. In the first one, a layer of coating is created at the substrate – the particle-substrate interactions responsible for adhesive bonding. Afterwards proper coating is deposited, i.e. the particle-coating interactions responsible for cohesive bonding. Appropriate selection of the
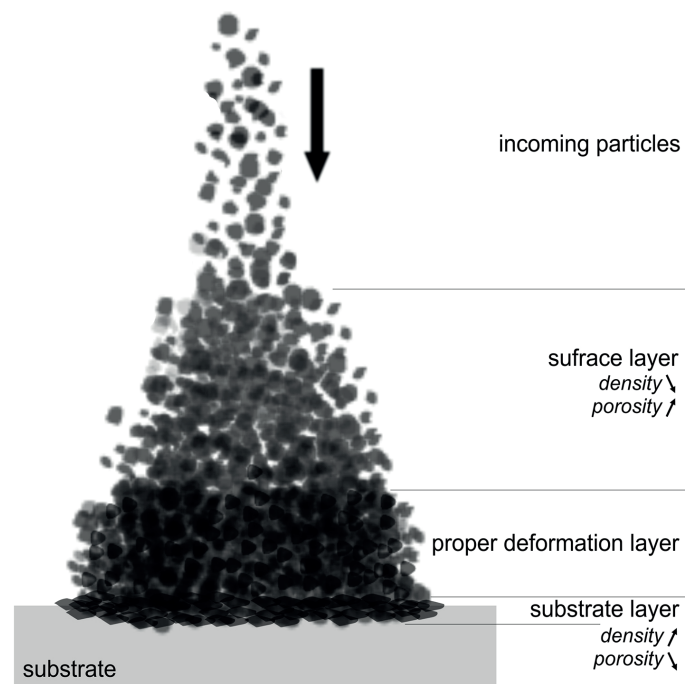

Fig. 6. Diagram of coating formation in the Cold Spraying process (inspired by [11])

substrate and the powder materials and preparation of the substrate surface are of key importance in the first stage [30]. It is recommended to heat the substrate prior to spraying, which will increase the energy of the process. In the second stage, the approaching particles hit previously deposited particles, deform and bind with each other. Preparation of the powder, its shape, temperature and the level of oxidation are of key importance at this stage. Even a highly oxidized powder can be deposited on a properly prepared substrate, however, the coating thus formed will be characterized by very poor adhesive and cohesive properties. As a result of the particles impacting each other, they are highly deformed, which decreases porosity in the coating [6].

During collision of the powder particles with the substrate, strong plastic deformation occurs. The oxide shell of a single particle cracks and is removed along with the emerging flash, both of the particle as well as of the substrate material. The flash allows for bonding metallically pure surfaces. The gas stream blows away residues of the oxide shell from the surface of the coating [11]. The manner of forming the particle on the substrate along with distribution of the stress fields created during the spraying is shown on the example of the impact of a Cu particle on a Cu substrate (Fig. 7). The greatest stresses occur in the contact zone and are closely dependent on the energy of the process (Fig. 7a). The higher velocity of the powder particles generates greater kinetic energy, leading to increased stresses and deformation during contact with the substrate. As a result, coating with higher density and better mechanical properties is obtained [31, 32]. The plastic deformation created in the particle and in the substrate is caused by large stresses occurring at the moment of impact, and is found mainly in the contact zone
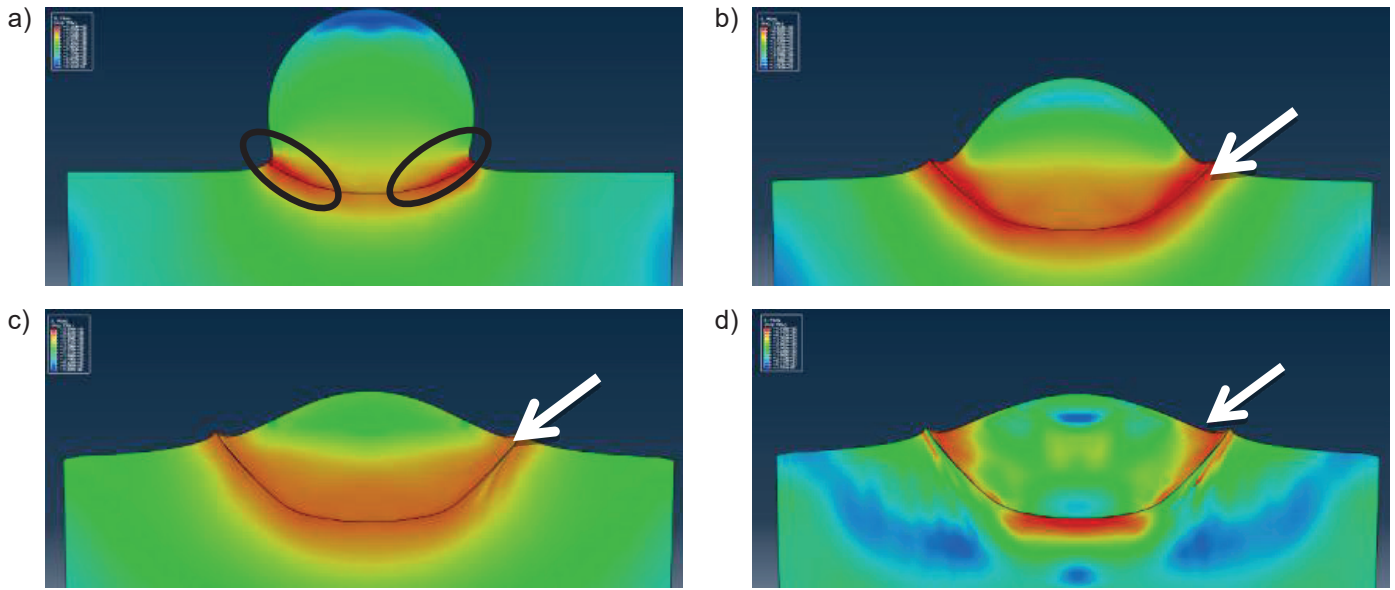
Fig. 7. Formation of a 20 μm Cu particle during spraying on a Cu substrate along with distribution of the stress field at various points in the process, after: 10 ns (a), 25 ns (b), 40 ns (c) and 50 ns (d) from the moment of contact. The arrow indicates the emerging material flash (own materials)

(Fig. 8a, b). There is visible flattening of the particle due to the impact, resulting in particle diameter reduction in the ratio of 2:3. The impact of subsequent particles increases the deformation of the first particle. Ultimately the particles in the coating obtain a flattened shape, in the ratio of even 1:5 as compared to initial particle diameter. As a result of such large deformations, an even greater creation of flash occurs [21, 33]. It is estimated that 90% of the plastic deformation energy is dispersed in the form of heat [7]. Additionally, the higher temperature of the process has a similar effect, because it leads to the thermal softening of the material [22]. The distribution of the temperature field is shown in Fig. 8c, d. Similarly to the deformation, the

temperature increase, occurs only in the contact zone of the particles with the substrate. The temperature value increases locally to a temperature close to the melting point, and in the presented example for copper it reaches about 1000°C. This is due to the appearance of shear stresses, which lead to the unstable adiabatic shear of the material.

Plastic deformation comes from the dislocation movements caused by the critical shear stress. It appears during impact into the substrate in all the grains of the microstructure of a single powder particle. The border surface of the particle may reduce the deformation of some grains. This indicates a different level of plastic deformation of the internal structure of a single par-
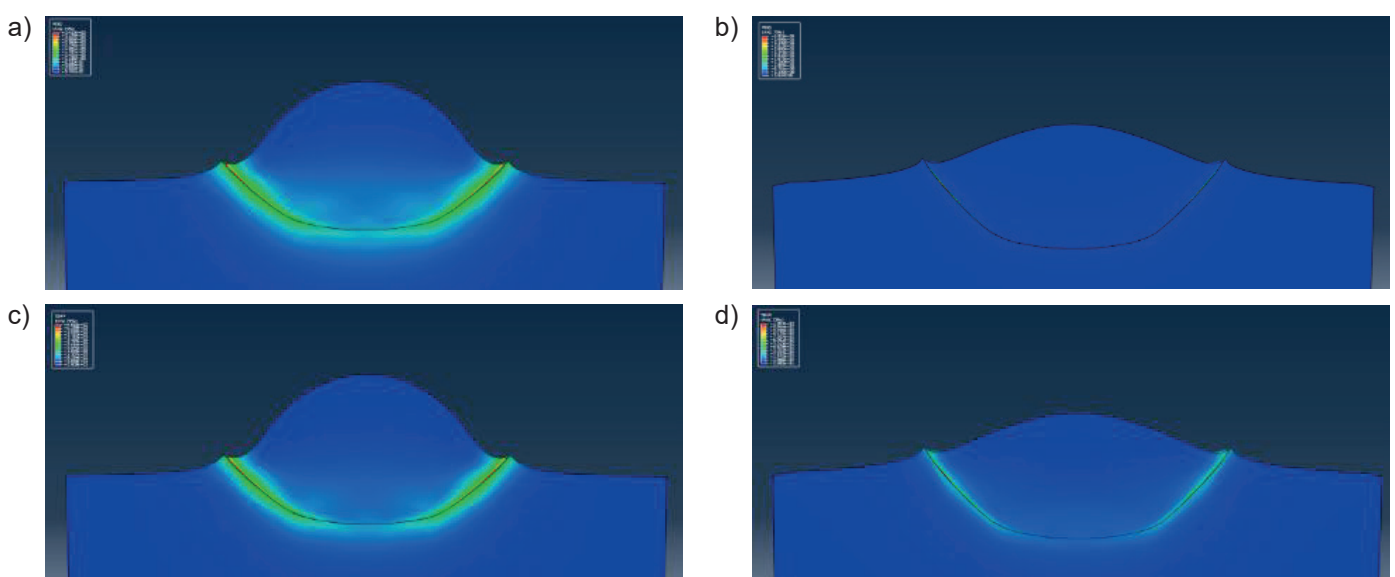

Fig. 8. Impact of a 20 μm Cu particle on a Cu substrate, distribution of deformation after 25 ns (a) and 50 ns (b), distribution of temperature field after 25 ns (c) and 50ns (d) (V = 450 m/s, $T_{particle}$ = 20°C, $T_{substrate}$ = 20°C) (own materials)

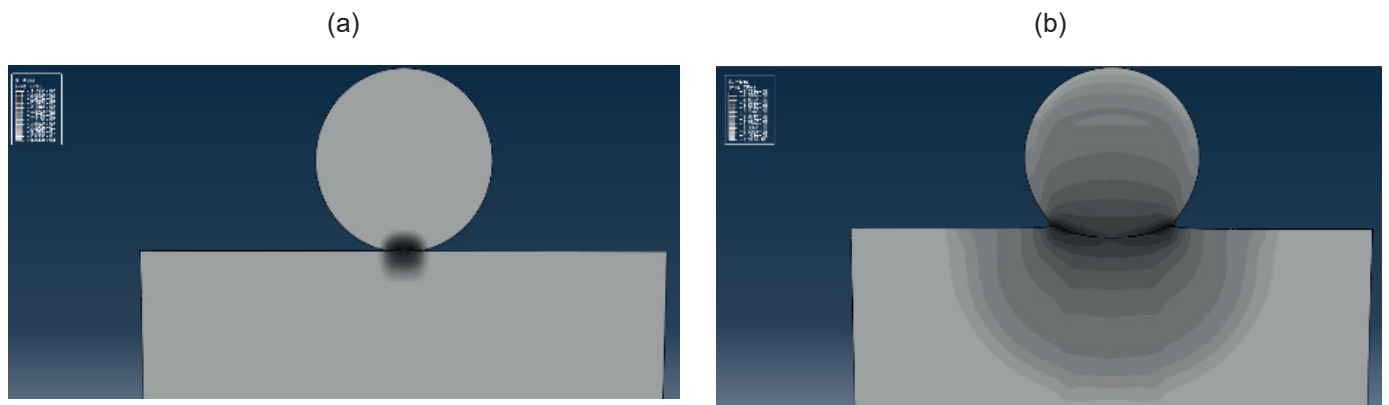(a)   (b)

Fig. 9. Spherical stress field during impact after 1 ns (a) and 5 ns (b) (own materials)

ticle and is thereby reflected in the microstructure of the whole coating [34]. As a result, strengthening of the material through deformation occurs. Due to the acquired hardness and strength, the material resists further deformation. The shear stresses resulting from the impact propagate spherically in the material of the particle and the substrate (Fig. 9) [7].

Deformation of the material in the solid state, with a high strain, leads to local heating of the material, which in turn causes adiabatic shear instability on the surface [19]. As a result of adiabatic shear instability and high impact energy, the materials of the particle and the substrate are moving on the surface relative to each other at different velocities and material flowing occurs. This phenomenon is accompanied by the rolling of the material in the interphase area. This type of material forming improves the bonding of the particle and substrate material in three ways: firstly, it significantly increases the interphase contact surface, then it causes local mixing of the materials and provides mechanical jamming of the particle with the substrate [11, 35]. Material flow causing the formation of local shear bands begins [19, 21]. This is accompanied by a local temperature increase to such a value that recrystallization occurs [35]. Moreover, the temperature value could locally reach the melting point of the material. As a result, intensive deformation occurs, material flash is created and very good bonding between the particles and the substrate is achieved. The phenomenon of local unstable adiabatic shear is characterized by a significant increase in temperature coupled with deformation and decrease in the stress over a very short period of time. Therefore higher velocity facilitates particle bonding.

The particle size, along with the surface temperature, stress and deformation rate, has a huge impact on the phenomenon of adiabatic shear. Small particles have a higher temperature gradient and therefore their shear instability can be inhibited by rapid cooling. Additionally, small particles are more easily strain-hardened due to high strain rates.

The way in which the particle impacts the substrate depends on the part of the stream in which it is located. In the axis of the stream, right by the substrate, there is the so-called stagnation point. Regardless of the arising shock wave, when a particle impacts the substrate at this point, it will be depos-

ited perpendicularly. If a particle is located further away from the axis, towards the boundary of the stream, then it will be deposited at a certain angle. The further away from the axis of the stream, the lower the efficiency of deposition [13]. At a certain point, the angle of the particles is so large, that they are not deposited on the substrate, but bounce off it (Fig. 10).
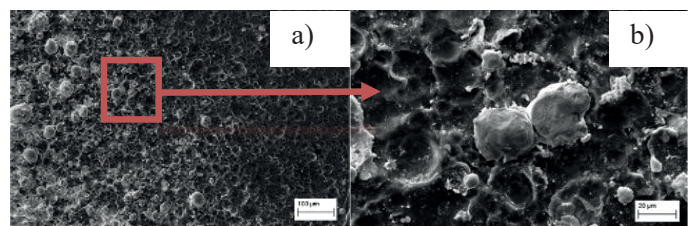

Fig. 10. SEM image of Sn particles deposited on a ground Al substrate, while located at the boundary of the stream (own materials)

With shear instability, a significant increase of temperature in a given area occurs, which causes material flow. Thus a sudden increase in the temperature of the deposited particles can be observed. It should be noted that in order to bond a particle with the substrate, a temperature must be generated with a value of at least 60% of the melting point of one of the materials [36].

The bonding mechanism occurs through intense local deformation of the material on the border between the particle and the substrate, which takes place during the impact on the substrate. Adhesive bonding depends on the size of the interphase boundary area. The adhesion, caused by van der Waals forces and the electrostatic force, usually occurs in the form of sticking [37]. During spraying, local metallurgical bonding may also occurs, caused by local softening of the material and diffusion [38]. Diffusion typically occurs at the substrate, where the intermetallic layer is formed with mixed materials of the powder and the substrate [39, 40]. Local melting of the material is possible for powders of metals with a low melting point, such as Sn, Zn and Al. A high temperature should then be used when heating the working gas [41].

4. Structures of coatings created with cold spray method

Granulation of the powder applied should be below 50 μm. This is due to the energy necessary for the deposition of a particle. Large particles have high mass, however, they obtain significantly lower velocities in the gas stream. In addition, the larger surface of the particle leads to greater oxidation, which is also disadvantageous. Large particles often bounce off the substrate, constituting a loss, hence they are only locally present in the coating being formed.

Results of our own study have shown that coatings deposited with the cold spray method have a strongly deformed structure, resulting from high plastic deformation. Therefore, the structure has the form of flattened ellipses with a flattening ratio of 3:1 or 5:1 [6]. The coatings typically exhibit high density and low porosity, but these properties ultimately depend on the sprayed material and the process parameters [42]. In some coatings areas of strong dislocation, elongated grains, twins and recrystallized grains can be observed, which indicates heterogeneous microstructure. What is more, Kairet et al. [43] noticed that copper coatings deposited with fine powder particles showed higher dislocation density as compared to large powder particles. Figure 11 presents the microstructure of a sample Cu coating, deposited with the LPCS method onto an Al substrate (Table 1). The high level of deformation of the particles is clearly visible. The density of the coating is very high. Additionally, high temperature is
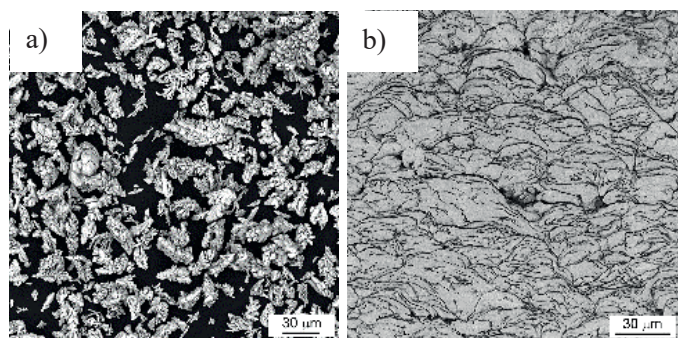

Fig. 11. Cu powder (a) and the coating obtained from its application in LPCS process (b) (own materials) (spraying parameters in Table 2)

Table 1
Spraying parameters

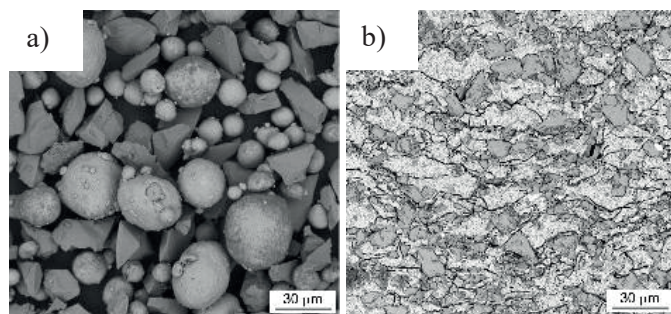| Coating	Powder feed rate [g/min]	Traverse speed υ_l [mm/s]	Gas pressure p_g [MPa]	Gas temperature T_g [°C]	Stand-off [mm]
Cu spherical	40	600	0.9	600	10
Cu dendritic	30	600	0.9	600	10
Cu+Al₂O₃	40	600	0.9	600	10
Sn	35	600	0.7	200	10
Sn + Al₂O₃	40	600	0.7	200	10
Al + Al₂O₃	45	600	0.7	400	10

Fig. 12. Al + Al$_2$O$_3$ powder mixture (a) and the coating obtained from its application in LPCS process (b) (own materials) (spraying parameters in Table 2)
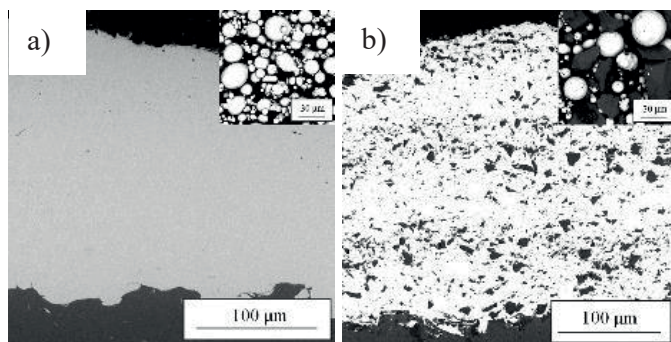

Fig. 13. SEM micrograph of LPCS coatings composed of spherical Cu (a) and mixture of spherical Cu and irregular Al$_2$O$_3$ (50 wt.% of Al$_2$O$_3$) (b) powders with the particle size of −50 + 10 μm (own materials) (spraying parameters in Table 1)

not involved in the spraying process, so the level of coating oxidation corresponds to that of the particles prior to spraying [11].

For comparison, Fig. 12 shows the microstructure of an Al+Al$_2$O$_3$ coating deposited with the LPCS method on a Cu substrate (Table 1). The coating is also characterized by low porosity, lack of oxidation and clear reinforcement with the ceramics particles. A comparison of Cu coatings deposited with the LPCS methods, with and without the addition of ceramics, is shown in Fig. 13.

The level of deformation depends strongly on powder material and the spraying parameters. Tin gas atomised powder deposited with a low spraying temperature of 200°C manifested low deformation combined with high coating density (Fig. 14a). However, adding ceramics to the powder caused an intensive tamping effect and flattening of tin particles in the coatings (Fig. 14b). Spraying of metal powders of higher mechanical properties, e.g. Ni, Ti, etc., without adding ceramics, causes lower plastic deformation. As a result, the coating deposited shows higher porosity, even when using the HPCS method (Fig. 15a) [44]. Adiabatic shear is significantly reduced, along with material deformation. However, powder particles are work-hardened and elongation of microstructure grains occurs (Fig. 15b).

An advantage of the cold spray process is the absence of material melting, which allows to avoid phase transformations and oxidation. It also usually helps avoid the formation of un-
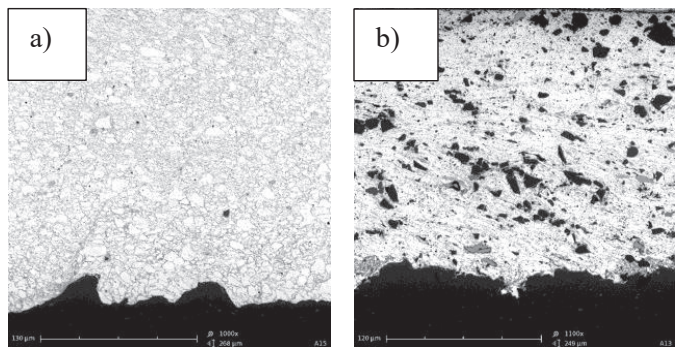
Fig. 14. SEM micrograph of LPCS coating composed of tin powder (a) and tin mixed with alumina (50 wt.% of Al_2O_3) (b) (spraying parameters in Table 1)
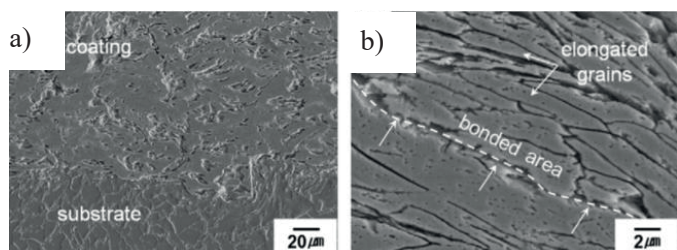

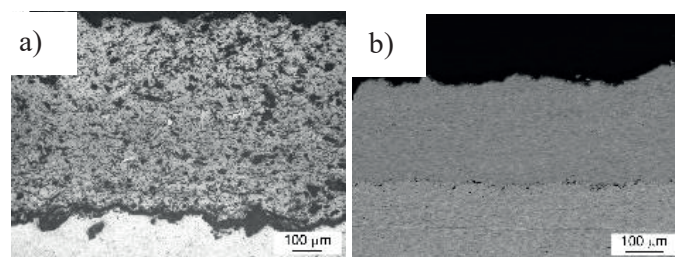Fig. 15. SEM micrograph of etched nickel coating (a, b) [50]

Fig. 16. SEM micrograph of copper coatings deposited onto aluminium substrate with the APS (a) and LPCS (b) methods (own materials)

desirable phases, although for some powders (Ni, Al) the presence of intermetallic or even nanocrystalline phases has been observed [45]. The comparison of copper coatings deposited with the same powder, but using different spraying methods, is shown in Fig. 16. Cu coating deposited with the air plasma spraying (APS) method (Fig. 16a) exhibits porosity of about 9% (black fields) and oxidation of 1.7% (dark-grey fields). Cu coating deposited by means of cold spraying using air exhibits porosity of about 1% without visible oxidation. Thus, probably coating oxidation is equivalent to the level of oxidation to be found in the powder. Due to the substantially lower temperatures of the process, the reaction of the metal with oxygen is significantly reduced [11].

5. Heat treatment of coatings

Heat treatment affects the microstructure of the coating through a number of mechanisms, depending on the temperature during the process. Recovery, recrystallization and grain growth occur

for different temperature ranges [46, 47]. Fragmentation of the structure following heat treatment, as a result of recrystallization, was also observed [4, 11, 46–48]. Additionally, heat treatment of a coating after spraying allows for relaxation of particles that exhibit a high level of deformation due to the strain. The example of an LPCS coating composed of dendritic copper powder with particle size of −45 + 10 µm and annealed for 2 hours in a protective atmosphere of H_2 at 400°C is shown in Fig. 17. The heat post-treatment clearly led to a reduction in the porosity of the coating and to particle relaxation. Additionally, heat treatment changed coating properties by increasing e.g. ductility [49] and electrical conductivity (Fig. 18).

The drawback of basic thermal-spraying methods, in which the material melts during the spraying process, is the presence of high residual stresses. Tensile residual stresses result from thermal contraction during the cooling of the coating from the solidification point, and may lead to cracks in the coating and even total separation from the substrate. Moreover, tensile residual stresses often limit the maximum thickness of the newly-created coating. In the methods using high kinetic energy, e.g. cold spray and HVOF, peening stress occurs along with thermal stresses. It is believed that it plays a dominant role in the cold spray process and frequently causes a compressive residual stress state following the deposition process. The experimentally determined distribution of residual stresses in an aluminium coating deposited on a polyamide 6 substrate
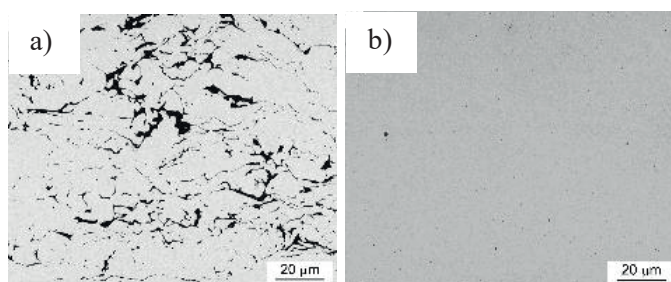
Fig. 17. SEM micrograph of a coating sprayed using the LPCS method (a) and subjected to heat treatment in a protective atmosphere of hydrogen (b) (own materials)

Fig. 18. Effect of heat treatment on electrical conductivity of Cu coatings deposited using various methods of thermal spraying: AS – arc spraying, APS – atmospheric plasma spraying, HVOF – supersonic spraying, LPCS – low pressure cold spraying, HPCS – high pressure cold spraying (CS). The heat treatment conditions are marked with numbers in the figure

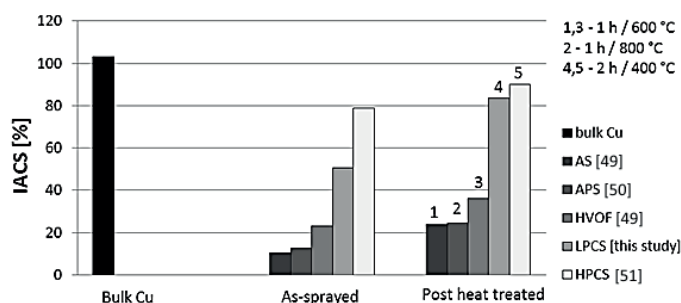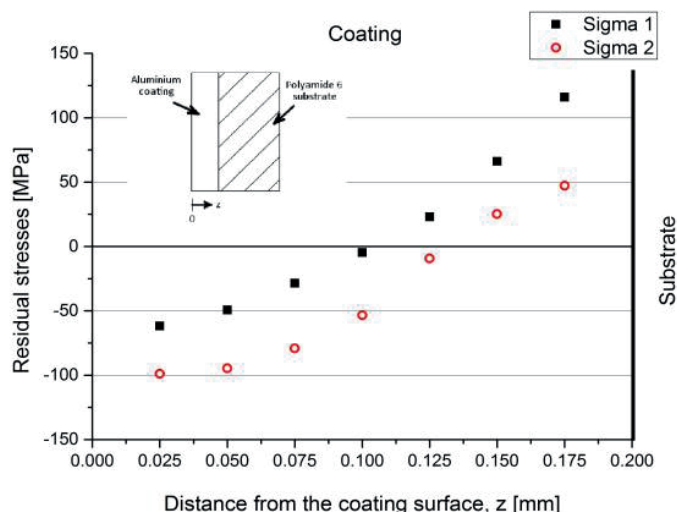Fig. 19. Experimentally determined distribution of residual stresses in aluminium coating on polyamide 6 deposited by means of the low pressure cold spraying method (own materials)

is shown in Fig. 19. The profile confirms that there are compressive stresses within the coating which then gradually turn into tensile stresses near the substrate. Due to the fact that the coating does not exhibit the presence of significant tensile stress values, there is no risk of cracking. Therefore when using the cold spray method, coatings of any thickness, even exceeding 10 cm, can be deposited [1].

6. Cold spraying methods

Cold spraying methods can be divided into two separate processes, i.e. the high pressure cold spraying (HPCS) method and the low pressure cold spraying (LPCS) method. In the HPCS process, nitrogen, helium or their mixtures at a pressure of 4 MPa and preheating temperature reaching up to 1100°C are typically used as the working gas. These parameters allow to obtain particle velocity in the range of 400–1200 m/s [7, 13, 28]. In the high pressure method, there is a greater choice of materials for spraying and those include in particular: Al, Cu, Cu-Sn, Ni, Ni-Cr, Ni-Al, Ta and Ti.

In the LPCS process, the working gas is either air or nitrogen at a pressure of 1 MPa and input temperature in the range from ambient temperature to 650°C. The obtained particle velocities are in the range of 300–700 m/s [4]. Because in the low-pressure method substantially lower velocities and temperatures are obtained, there is considerable limitation of the sprayed materials to just Sn, Zn, Al, Cu and Ni. In order to increase the efficiency of the process and improve the properties of the finally obtained coating, it is recommended to use a ceramics admixture (Al$_2$O$_3$, SiC) for the input metal powder. This allows to create cermet coatings. The amount of the ceramics added to the metal powder is a key factor affecting the adhesion of coatings in the case of the low-pressure method. It serves three functions: that of preventing clogging of the nozzle, activating the surface by

removing oxides and compacting the powder particles of the metal. This is due to the irregular shape and higher velocities of the ceramic particles in the gas stream [4, 22]. The ceramic particles mixed with metal particles remove the layer of oxide from the surface of the substrate and from the surface of the particles, during the impact at the substrate or collisions occurring still in the gas stream [50]. Therefore, along with an increase in the content of ceramics in the powder, the mechanical properties of the coating are greatly improved [4, 51–62]. What is more, adding ceramics changes the type of fracture, from adhesive to cohesive, observed in the peel tests of aluminium coating [56]. The most favourable properties have been observed in the case of 50% volume Al$_2$O$_3$ ceramics addition [4].

Table 2 lists the spraying parameters for the HPCS and LPCS processes. Higher parameters of the HPCS process allow to achieve significantly higher efficiency of the spraying process, exceeding even 90%, whereas in the LPCS process it reaches only about 60%. However, the costs of the HPCS process are incomparably higher. Attention should be paid in particular to the gas flow rate and the powder mass concentration. At maximum parameters, the HPCS process is particularly expensive.

Table 2
Comparison of spraying parameters in HPCS and LPCS processes [1, 4, 11]

Parameter	HPCS	LPCS
Working gas	N$_2$, He, mixture	air, N$_2$
Gas pressure (MPa)	1–5	0.1–1
Gas temperature (°C)	20–1100	20–650
Gas flow rate (m^3/min)	0.85–2.5 (N$_2$), max. 4.2 (He)	0.3–0.4
Powder mass concentration (kg/h)	4.5–13.5	0.3–3
Spraying distance (mm)	10–50	5–15
Electrical power (kW)	17–47	3.3
Particle size (μm)	5–100	10–50

7. Summary

Cold spraying is one of the most often analysed thermal-spraying method in the literature. This arises from its main advantage – deposition of high purity metal coatings, which might improve various parameters of the substrate material, e.g. corrosion resistance, wear resistance and high temperature resistance as well as electrical and thermal conductivity. What is more, cold spray is also applied to regenerate damaged parts or improve their appearance. In the manuscript, according to authors' research and the recently published literature, theoretical aspects of the cold spraying process are presented. It is worth stressing that cold spraying is a solid state particles deposition process. Powder particles are heated by working gas in the stagnation section of the nozzle and next cooled in the divergent part of nozzle. Simultaneously, powder particles gain supersonic velocity in the nozzle. As a result of impact onto the substrate, with high ki-

netic energy, particles deform plastically and form a coating by means of mechanical interlocking or diffusion. Finally, uniform coating is created with low porosity and oxidation comparable to that of the powder used.

The most important process parameters in cold spraying are particle velocity and temperature. High particle velocity in the gas stream provides intensive plastic deformation, while high particle temperature increases material plasticity. Therefore, with optimum process parameters, dedicated for the material selected, dense coating with high bond strength can be obtained.

The cold spraying method provides significant advantages: (i) the setup in LPCS method is mobile and can be used in the exact location where coating is being applied, e.g. in the case of a bridge renovation, (ii) the process utilization is not limited by part size, shape or dimension, etc., (iii) various coating shapes can be obtained by using masking frames or machining of as-sprayed coatings, (iv) it is possible to form very thick coatings of several centimetres, which can be compared to additive technologies, (v) spraying does not cause substrate melting. However, there are also some disadvantages. The most important of those is the deposition efficiency, which depends strongly on powder material properties. Thus the process can generate high costs in selected applications.

It should be emphasized that cold spraying is a very interesting technique for functional coatings deposition which can find its application in many industrial fields. Despite current problems with deposition of selected materials, cold spraying continues to be developed by researchers all over the world. Therefore, it can be suspected that in the future it will find further applications for new materials and in new fields.

References

[1] A. Papyrin, V. Kosarev, S. Klinkov, A. Alkimov, and V. Fomin, *Cold Spray Technology*, Elsevier, 2007.

[2] M. Grujicic, C. Zhao, C. Tong, W. DeRosset, and D. Helfritch, "Analysis of the impact velocity of powder particles in the cold-gas dynamic-spray process", *Mat. Sci. Eng. A* 368, 222–230 (2004).

[3] R. Dykhuizen and M. Smith, "Gas dynamic principles of cold spray", *J. Therm. Spray Technol.* 7, 205–212, (1998).

[4] R. Maev and V. Leshchynsky, "Air gas dynamic spraying of powder mixtures: Theory and application", *J. Therm. Spray Technol.* 15, 198–205 (2006).

[5] T. Stoltenhoff, H. Kreye, and H. Richter, "An analysis of the cold spray process and its coatings", *J. Therm. Spray Technol.* 11, 542–550 (2001).

[6] T. Van Steenkiste, J. Smith, and R. Teets, "Aluminum coatings via kinetic spray with relatively large powder particles", *Surf. Coat. Technol.* 154, 237–252 (2002).

[7] T. Schmidt, F. Gärtner, H. Assadi, and H. Kreye, "Development of a generalized parameter window for cold spray deposition", *Acta Mater.* 54, 729–742 (2006).

[8] T. Han, Z. Zhao, B. Gillispie, and J. Smith, "A fundamental study of the kinetic spray process", *Thermal Spray 2004: Advances in Technology and Application*, Osaka, ASM International (2004).

[9] S. Shin, S. Yoon, Y. Kim, and C. Lee, "Effect of particle parameters on the deposition characteristics of a hard/soft-particles composite in kinetic spraying", *Surf. Coat. Technol.* 201, 3457–3461 (2006).

[10] P. Sudharshan Phani, D. Srinivasa Rao, S. Joshl, and G. Sundararajan, "Effect of process parameters and heat treatments on properties of cold sprayed copper coatings", *J. Therm. Spray Technol.* 16, 425–434 (2007).

[11] V. Champagne, *The Cold Spray Materials Deposition Process: Fundamentals and Applications*, Woodhead Publishing Ltd., Cambridge, 2007.

[12] R. Maev and V. Leshchynsky, *Introduction to Low Pressure Gas Dynamic Spray*, Physics & Technology, Wiley-VCH Verlag GmbH&Co, KGaA, Weinheim, 2008.

[13] T. Schmidt, H. Assadi, F. Gärtner, H. Richter, T. Stoltenhoff, H. Kreye, and T. Klassen, "From particle acceleration to impact and bonding in cold spraying", *J. Therm. Spray Technol.* 18, 794–808 (2009).

[14] T. van Steenkiste and J.R. Smith, "Evaluation of coatings produced via kinetic and cold spray processes", *J. Therm. Spray Technol.* 13, 274–282. (2004).

[15] M. Faizan-Ur-Rab, S.H. Zahiri, S.H. Masood, T.D. Phan, M. Jahedi, and R. Nagarajah, "Application of a holistic 3D model to estimate state of cold spray titanium particles", *Materials and Design* 89 1227–1241 (2016).

[16] V. Kosarev, S. Klinkov, A. Alkhimov, and A. Papyrin, "On some aspects of gas dynamics of the cold spray process", *J. Therm. Spray Technol.* 12, 265–281 (2003).

[17] B. Jodoin, "Effects of Shock Waves on Impact Velocity of Cold Spray Particles", in: *Thermal Spray 2001: New Surfaces for a New Millennium*, C. Berndt, K. Khor, E. Lugscheider (Eds.), May 28–30 (Singapore), ASM International, pp. 399–407.

[18] J. Pattison, S. Celotto, and A. Khan, W. O'Neill, "Standoff distance and bow shock phenomena in the cold spray process", *Surf. Coat. Technol.* 202, 1443–1454 (2008).

[19] M. Meyers, "Plasticity: Adiabatic shear localization", *Encyclop. Mat.: Sci. Technol.* 7093–7103.

[20] C.-J. Li and W.-Y. Li, "Examination of the critical velocity for deposition of particles in cold spraying", *Thermal Spray 2005: Explore its surfacing potential*, ASM International, pp. 217–224 (2005).

[21] D. Helfritch and V. Champagne, "Optimal particle size for the cold spray process", *Thermal Spray 2006: Building on 100 Years of Success*, ASM International, (2006).

[22] H. Assadi, F. Gärtner, T. Stoltenhoff, and H. Kreye, "Bonding mechanism in cold gas spraying", *Acta Mater.* 51, 4379–4394 (2003).

[23] P. Richter and H. Höll, "Latest technology for commercially available cold spray systems", *Thermal Spray 2006: Building on 100 Years of Success*, ASM International, (2006).

[24] C. Borchers, F. Gärtner, T. Stoltenhoff, H. Assadi, and H. Kreye, "Microstructural and macroscopic properties of cold sprayed copper coatings", *J. Appl. Phys.* 93, 10064–10070, (2003).

[25] S. Zumdahl, *Chemical Principles*, Houghton Mifflin Company, Boston, New York, 1998.

[26] X.-J. Ning, J.-H. Jang, and H.-J. Kim, "The effects of powder properties on in-flight particle velocity and deposition process during low pressure cold spray process", *Appl. Surf. Sci.* 253, 7449–7455 (2007).

[27] H. Katanoda, M. Fukuhara, and N. Iino, "Numerical study of combination parameters for particle impact velocity and temperature in cold spray", *J. Therm. Spray Technol.* 16, 627–633 (2007).

[28] A. Alkhimov, S. Klinkov, and V. Kosarev, "Experimental study of deformation and attachment of microparticles to an obstacle upon high-rate impact", *J. Appl. Mech. Tech. Phy.* 41, 245–250 (2000).

[29] K. Kang, S. Yoon, Y. Ji, and C. Lee, "Oxidation effects on the critical velocity of pure Al feedstock deposition in the kinetic spraying process", *Thermal Spray 2007: Global Coating Solutions*, ASM International, (2007).

[30] A. Papyrin, S. Klinkov, and V. Kosarev, "Effect of the substrate surface activation on the process of cold spray coating formation", *Thermal Spray 2005: Explore its surfacing potential*, Basel, ASM International, 145–150 (2005).

[31] T. Van Steenkiste and D. Gorkiewicz, "Analysis of tantalum coatings produced by the kinetic spray process", *J. Therm. Spray Technol*. 13, 265–273 (2004).

[32] T. Price, P. Shipway, D. McCartney, E. Calla, and D. Zhang, "A method for characterizing the degree of inter-particle bond formation in cold sprayed coatings", *J. Therm. Spray Technol*. 16, 566–570 (2007).

[33] T. Schmidt, Kaltgasspritzen, *Eine Analyse des Materialverhaltens beim Partikelaufprall und die daraus abgeleitete Prozessoptimierung*, Werkstofftechnik, Shaker Verlag, Hamburg, Germany, 2007.

[34] T.H. Courtney, *Mechanical Behavior of Materials*, McGrae-Hill Publishing Company, Singapore, 2000.

[35] M. Grujicic, J.R. Saylora, D.E. Beasleya, W.S. DeRossetb, and D. Helfritch, "Computational analysis of the interfacial bonding between feed-powder particles and the substrate in the cold-gas dynamic-spray process", *Appl. Surf. Sci.*, 219, 211–227 (2003).

[36] S. Yin, X.-F. Wang, W.-Y. Li, and X.-P. Guo, "Examination on substrate preheating process in cold gas dynamic spraying", *J. Therm. Spray Technol*, 20, 852–859 (2011).

[37] S. Klinkov, V. Kosarev, and M. Rein, "Cold spray deposition: Significance of particle impact phenomena", *Aerosp. Sci. Technol*. 9, 582–591 (2005).

[38] T. Hussain, D. McCartney, P. Shipway, and D. Zhang, "Bonding mechanisms in cold spraying: The contributions of metallurgical and mechanical components", *J. Therm. Spray Technol*. 18, 364–379 (2009).

[39] T. Kairet, "A contribution to the study of cold gas dynamic spraying of copper: Influence of the powder characteristics on the mechanical properties of the coating", PhD Thesis, Université Libre de Bruxelles, Belgium, 2007.

[40] S. Guetta, M. Berger, F. Borit, V. Guipont, M. Jeandin, M. Boustie, Y. Ichikawa, K. Sakaguchi, and K. Ogawa, "Influence of particle velocity on adhesion of cold-sprayed splats", *J. Therm. Spray Technol*. 18, 331–342 (2009).

[41] W.-Y. Li, C. Zhang, X. Guo, C.-J. Li, H. Liao, and C. Coddet, "Study on impact fusion at particle interfaces and its effect on coating microstructure in cold spraying", *Appl. Surf. Sci.*, 254, 517–526 (2007).

[42] A. Rezaeain, R. Chromik, S. Yue, E. Irissou, and J.-G. Legoux, "Characterization of cold-sprayed Ni, Ti and Cu coating properties for their optimizations", *Thermal Spray 2008: Thermal Spray Crossing Borders*, E. Lugscheider (Ed.), June 2–4 (Maastricht, The Netherlands), DVS, 854–860.

[43] T. Kairet, G. Di Stefano, M. Degrez, F. Campana, and J.-P. Janssen, "Comparison Between Coatings from two Different Copper Powders: Mechanical Properties, Hardness and Bond Strength", *Thermal Spray 2006: Building on 100 Years of Success*, B. Marple, M. Hyland, Y.-C. Lau, R. Lima, J. Voyer (Eds.), May 15–18 (Seattle, Washington, USA), ASM International.

[44] G. Bae, J. Jang, and Ch. Lee, "Correlation of particle impact conditions with bonding, nanocrystal formation and mechanical properties in kinetic sprayed nickel", *Acta Materialia* 60, 3524–3535 (2012).

[45] A. Bolesta, V. Fomin, M. Sharafutdinov, and B. Tolochko, "Investigation of interface boundary occurring during cold gas-dynamic spraying of metallic particles", *Nucl. Instrum. Methods Phys. Res., Sect. A* 470, 249–252 (2001).

[46] F. Gärtner, T. Stoltenhoff, J. Voyer, H. Kreye, S. Riekehr, and M. Kocak, "Mechanical properties of cold-sprayed and thermally sprayed copper coatings", *Surf. Coat. Technol*. 200, 770–6782 (2006).

[47] S. Semiatin, "Recovery, recrystallization, and grain-growth structures", *Metalworking: Bulk Forming* 14A, ASM Handbook, ASM International, 552–562 (2005).

[48] P.S. Phani, D.S. Rao, S.V. Joshi, and G. Sundararajan, "Effect of process parameters and heat peer reviewed treatments on properties of cold sprayed copper coatings", *J. Therm. Spray Technol*. 16, 425–434 (2007).

[49] T. Stoltenhoff, C. Borchers, F. Gärtner, and H. Kreye, "Microstructures and key properties of cold-sprayed and thermally sprayed copper coatings", *Surf. Coat. Technol*. 200, 4947 – 4960 (2006).

[50] L. Pawłowski, *The Science and Engineering of Thermal Spray Coatings*, John Wiley & Sons Ltd., New York, 2008.

[51] H. Koivuluoto, A. Coleman, K. Murray, M. Kearns, and P. Vuoristo, "High pressure cold sprayed (HPCS) and low pressure cold sprayed (LPCS) coatings prepared from OFHC Cu feedstock: Overview from powder characteristics to coating properties", *Journal of Thermal Spray Technology* 21, 1065–1075 (2012).

[52] M. Decker, R. Neiser, D. Gilmore, and H. Tran, "Microstructure and Properties of Cold Spray Nickel", *Thermal Spray 2001: New Surfaces for a New Millennium*, C. Berndt, K. Khor, E. Lugscheider (Eds.), May 28–30 (Singapore), ASM International, 433–439 (2001).

[53] S. Klinkov, V. Kosarev, A. Sova, and I. Smurov, "Calculation of particle parameters for cold spray spraying of metal-ceramic mixtures", *J. Therm. Spray Technol*. 18, 944–956 (2009).

[54] L. Pawłowski, *The Science and Engineering of Thermal Spray Coatings*, John Wiley & Sons Ltd., New York, 2008.

[55] H. Koivuluoto, J. Lagerbom, M. Kylmalahti, and P. Vuoristo, "Microstructure and mechanical properties of low-pressure cold-sprayed (LPCS) coatings", *J. Therm. Spray Technol*. 17 (5–6), 721–727 (2008).

[56] H. Mäkinen, J. Lagerbom, and P. Vuoristo, "Adhesion of cold sprayed coatings: Effect of powder, substrate, and heat treatment", *Thermal Spray 2007: Global Coating Solutions: Proceedings of the 2007 International Thermal Spray Technology*, Beijing, (2007).

[57] X.-J.Ning, J.-H. Kim, H.-J. Kim, and C. Lee, "Characteristics and heat treatment of cold-sprayed Al–Sn binary alloy coatings", *Appl. Surf. Sci*. 255, 3933–3939 (2009).

[58] H. Koivuluoto and P. Vuoristo, "Effect of powder type and composition on structure and mechanical properties of Cu + Al_2O_3 coatings prepared by using low-pressure cold spray process", *J. Therm. Spray Technol*. 19 (5), 1081–1092 (2010).

[59] Q. Wang, K. Spencer, N. Birbilis, and M.-X. Zhang, "The influence of ceramic particles on bond strength of cold spray composite coatings on AZ91 alloy substrate", *Surf. Coat. Technol*. 205, 50–56 (2010).

[60] K. Spencer, D.M. Fabijanic, and M.-X. Zhang, "The use of Al–Al O cold spray coatings to improve the surface properties of magnesium Alloys", *Surf. Coat. Technol*. 204, 336–344 (2009).

[61] E. Irissou, J.-G. Legoux, B. Arsenault, and Ch. Moreau, "Investigation of Al-Al2O3 cold spray coating formation and properties", *J. Therm. Spray Technol*. 16 (5–6), 661–668 (2007).

[62] H. Koivuluoto and P. Vuoristo, "Effect of ceramic particles on properties of cold-sprayed Ni-20Cr + Al_2O_3 coatings", *J. Therm. Spray Technol*. 18 (4), 555–562 (2009).